Aerosol Science 35 (2004) 805–821

Journal of
Aerosol Science

www.elsevier.com/locate/jaerosci

Microparticle detachment from surfaces exposed to turbulent air flow: Effects of flow and particle deposition characteristics

A.H. Ibrahim, P.F. Dunn*, R.M. Brach

Particle Dynamics Laboratory, Department of Aerospace and Mechanical Engineering, University of Notre Dame, Hessert Center Notre Dame, IN 46556, USA

Received 28 August 2003; received in revised form 16 December 2003; accepted 9 January 2004

Abstract

This work presents the results of experiments conducted to provide quantitative information on particle detachment from surfaces. The effects of certain, controllable factors on the detachment of 70 μm-diameter stainless-steel spheres from a glass surface exposed to accelerated air flow in a wind tunnel were studied. Changes in the free-stream velocity required to detach 50% of the particles, the threshold velocity for detachment, were measured for variations in the controlled factors. These factors were air relative humidity, residence time between particle deposition onto the substrate and flow application, mean flow acceleration, deposition density, final free-stream velocity, and final flow Reynolds number. Results reveal that deposition density was the most effective factor that enhanced detachment at all relative humidities. Residence time was found to be the most effective factor that suppressed detachment at high relative humidity. The threshold velocity increased with increasing relative humidity and was lower for turbulent flow versus laminar flow. Within the uncertainty limits, the mean flow acceleration in the transient period was found not to affect the threshold velocity in the range from 0.014 to 0.34 m/s^2. The final free-stream velocity also did not affect the threshold velocity, provided it was greater than the threshold. A set of experimental conditions that lead to a relatively small uncertainty is presented.

Keywords: Microparticles; Detachment; Surfaces; Flow

1. Introduction

Resuspension of particles from surfaces due to turbulent flow occurs in many situations. For example, smoke and soot particulates can deposit on particles. These particles can be detached from the surfaces, reentrained into the circulating air and eventually respired into the lungs. Contaminant

* Corresponding author.
E-mail address: pdunn@nd.edu (P.F. Dunn).

0021-8502/$ - see front matter © 2004 Elsevier Ltd. All rights reserved.
doi:10.1016/j.jaerosci.2004.01.002

particles can detach from internal pipe surfaces during the production of ultra-pure gases (Wen, Kasper, & Udischas, 1989). Extensive reviews on the resuspension of particles from surfaces have been made by Ziskind, Fichman, and Gutfinger (1995), Sehmel (1980), and Nicholson (1988). Wang (1991) studied the effects of substrate cleanliness, deposition technique, storage duration up to 48 days and moisture concentration on the removal of microparticles from surfaces and suggested a standard set of experimental conditions to minimize uncertainty. Many detachment and resuspension experiments, however, have been conducted under a variety of conditions and there is a need to investigate the effects of changes in these factors on detachment.

Typically, in detachment experiments, the flow velocity is increased with time over an initial transient period until a steady mean velocity is reached. It is unknown, however, whether or not the mean flow acceleration during this transient period affects the detachment behavior. In addition, different investigators have used different values of relative humidity, residence time between deposition and application of the flow, during which relative humidity can change, deposition density (initial number of particles per unit area of the field of view, N_0), final free-stream velocity, U_∞, and Reynolds number, Re. The large scatter in the resuspension data can be due to the different ranges in these factors. For example, the reported values of resuspension rates range over more than six orders of magnitudes (Sehmel, 1980).

Ibrahim, Dunn, and Brach (2003) presented experiments for the detachment of spherical and irregular particles, ranging from 10 to 65 μm in diameter, from a glass substrate under controlled conditions. They obtained relatively small variability by carefully controlling the experimental conditions and the substrate preparation technique. They showed that the threshold velocity for detachment, U_{th}, can be estimated based on incipient motion occurring as pure rolling.

The present work investigates the effects of several flow and particle deposition characteristics on the detachment behavior. It provides quantitative information about these effects under controlled experimental conditions.

In the following, the experimental procedure is described first. Then the experimental results are presented and analyzed. Finally, the results are summarized with suggestions on effective ways either to enhance or to suppress detachment. Most of the experiments presented here are for turbulent flow, with only one laminar flow experiment to investigate the effects of this regime.

2. Description of experiments

A schematic of the experimental facility is shown in Fig. 1. Air is drawn through a contraction section containing 12 screens (1.05 m long; contraction ratio 27:1), an inlet section (1 m long; distributed roughness element at its beginning to produce boundary layer turbulence), a test section (1 m long; 20.3 cm × 20.3 cm) and a diffuser section (1.05 m long; four-blade fan and 7.5 HP motor). The wind tunnel is equipped with a programmable controller to set the acceleration during the transient phase and the final, steady-state velocity. The diffuser is equipped with a type-K thermocouple and a relative humidity sensor. Both are connected to a voltage amplifier and data-acquisition board (National Instruments 6034E).

The test section includes a smooth flat plate at its bottom that is 1.05 m long with a leading wedge angle of 10°. The flat plate contains a grove designed to accommodate a glass substrate (Amersham Pharmacia; 10 cm width × 10.5 cm length × 1.27 mm thickness).

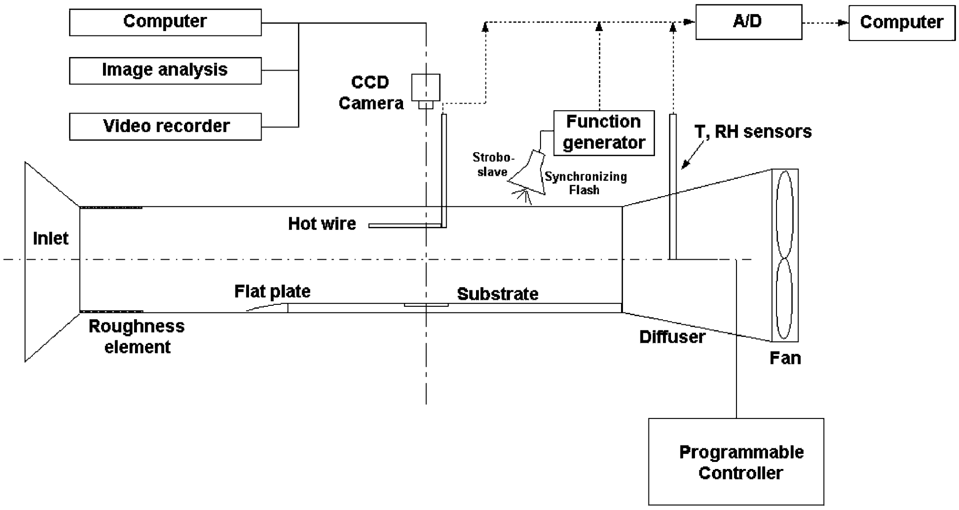

Fig. 1. Schematic of the wind tunnel used to study particle detachment.

The free-stream velocity can be varied from zero up to approximately 24 m/s. The flow velocity is accelerated from zero up to the prescribed steady-state velocity almost linearly with time. Flow cross-sectional and length-wise developments have been assessed using single hot-wire anemometry and are controllable to within 5%. Transient profiles are repeatable to within 3%. Free stream turbulence intensity is less than 1% over the entire velocity range. The motion of the particles is recorded using a 30 frames/s CCD camera (Astrovid 2000). Optical lenses (Olympus) are attached to the camera to achieve enough magnification (typically about $20\times$) to resolve individual particle motion. The camera output is connected to a digitizer and a frame grabber in a personal computer for image analysis. The field of view is $13.7\ \text{mm} \times 10.2\ \text{mm}$ for most cases.

Microvideographic images and free-stream velocity measurements are obtained simultaneously. The image acquisition is synchronized with the velocity measurement by a flash. Consequently, the number of particles on the surface is known at any time as a function of free-stream or friction velocity. The properties of the particle and surface are summarized in Table 1.

All experiments were conducted at 23 ± 2 °C and at different relative humidities. The particles were deposited as a monolayer on the glass substrate to avoid any cohesive forces between the particles. All particles were deposited by gravitational settling from a height of approximately 5 cm, resulting in elastic deformation upon contact with the substrate. No deposition was made upstream of the field of view. Deposition was made immediately before initiation of the flow, except when the effect of residence time was studied. The same deposition pattern and deposition density of deposited particles were followed, except when the collision effects were investigated. Most of the particles ($> 90\%$) were deposited as singlets and were not positioned in front of each other in the stream-wise direction. The deposition of deposited particles was such that it was large enough to achieve a monolayer with acceptable statistical accuracy but not too large to cause an unacceptable number of collisions on the surface. This amounted to depositing, on the average, approximately 70 particles over the field of view, resulting in a particle deposition density, N_0, of approximately

Table 1
Properties of the materials used

Property	Microparticles	Substrate
Material	Stainless steel, type 316	Glass
Manufacturer	Duke Scientific	Amersham Pharmacia
Dimensions	70 ± 6 μm diameter	10 cm × 10.5 cm × 1.27 mm
Density (kg/m^3)	8000	2420
Poisson's ratio	0.28	0.27
Young's modulus (GPa)	215	80.1
Surface energy of adhesion (J/m^2)	0.15	

The properties are obtained from the manufacturers and from Reeks, Reed, and Hall (1988).

0.5 particles/mm^2. Any particles detached by collisions were excluded from the manual count, which typically was about 7% of the total detached particles. The particles resided completely within the viscous sublayer of the boundary layer.

Similar glass substrates were used during the experiments and one of the substrates was scanned by an atomic force microscope. The mean of the standard deviations of asperity heights was 17 Å. The histogram of the asperity heights is shown in Ibrahim et al. (2003). Cheng, Brach, and Dunn (2002) found that this standard deviation of heights corresponds to a ratio of rough-to-smooth pull-off forces, C, of approximately 1%. Caylor (1993) examined a sample of the stainless-steel microspheres using a scanning electron microscope and found that their surface was smooth to within the resolution of the instrument.

For turbulent flow experiments, a distributed roughness element was used at the inlet section to trigger the boundary layer to turbulence. The measurements were made at a downstream distance of 1.4 m. Boundary layer velocity profiles were scanned at different velocities with a hot-wire probe and good agreement was found with the data of Klebanoff (1954). In addition, the friction velocity, u^* (defined as $\sqrt{\tau_w/\rho}$, where τ_w is the wall shear stress and ρ is the air density), was statically calibrated against the free-stream velocity, U_∞, as described in Ibrahim et al. (2003) and matched the empirical formulae for fully developed turbulent flow (Schlichting, 1979). The free-stream and friction velocities (m/s) are correlated through a least-squares linear regression by the equation

$$u^* = 0.0375U_\infty + 0.0387, \tag{1}$$

where the uncertainty is ± 0.0300 m/s at a 95% confidence level.

For laminar flow experiments, the distributed roughness element was removed and the measurements were made at a downstream distance of 0.14 m. Boundary layer velocity profiles were scanned at different velocities with a hot-wire probe to confirm agreement with the Blasius profile. The friction velocity was statically calibrated against the free-stream velocity using the measured boundary layer profiles. It was found to be within ±3% from the theoretical laminar friction velocity (Schlichting, 1979). The use of the friction velocities to characterize resuspension and detachment experiments allows for a comparison between experiments to be made at different flow configurations.

In the following, when the values of the factors are not mentioned, they were as follows: deposition was made immediately before initiation of the flow; the flow acceleration was 0.18 m/s^2; N_0 was approximately 0.5 particle/mm^2 and the flow was turbulent.

3. Experimental results

The experimental results are presented as detachment fraction versus free-stream velocity. This fraction is defined as

$$n^*(t) = 1 - \frac{n(t)}{n(0)}, \tag{2}$$

where $n(t)$ is the number of non-detached particles on the surface at time t.

It was observed that the particles detach over a range of velocities rather than at a single velocity. This is due to the inherent scatter in the particle size, surface roughness and surface and particle properties and the random nature of the turbulent fluid flow. In the present work, a threshold velocity for detachment, U_{th}, which was the velocity at which the detachment fraction equals 0.50, is selected to represent the overall detachment behavior.

3.1. Effects of relative humidity

The detachment rate is reduced at high relative humidity due to the increase of the pull-off force. Corn (1961) and Corn and Stein (1965) found almost no change in adhesion forces with relative humidities up to 30% and a rapid increase after that. Despite the large dependence of the detachment on relative humidity, many researchers do not report its value and many experiments are made under conditions corresponding to different values of relative humidity, thereby adding more uncertainty to the results. Ando (2000) measured the pull-off force between the tip of atomic force microscope probe and asperities on a silicon wafer at different relative humidities. He found that the pull-off force on a single asperity did not change with relative humidity. However, the pull-off force increased with relative humidity when contact was with an array of asperities. These findings suggest that the water adsorbed within the interface asperities increases the effective contact area and, consequently, the pull-off force. Some measurements have been made (for example, Zimon, 1980; Podczeck, Newton, & James 1997; Quon, Ulman, & Vanderlick, 2000; Ando, 2000) showing the increase of the pull-off force with the relative humidity.

The increase in the pull-off force with relative humidity causes an increase in the U_{th}. However, unlike the large amount of published results on the increase of the pull-off force versus the relative humidity, very few experiments have measured the increase in the U_{th} due to relative humidity. This subsection presents some quantitative information about this.

Fig. 2 shows the detachment fraction versus free-stream velocity for relative humidities of 18%, 25%, 30%, 36%, 48%, 61% and 67%. The corresponding U_{th}'s were 3.6, 3.6, 4.2, 5.0, 8.5, 10.7 and 13.4 m/s, respectively. It was necessary to increase the final free-stream velocities as the relative humidity increases to reach to a detachment fraction of at least 0.8. This amounted to using final free-stream velocities of 7.3, 7.3, 7.3, 7.3, 11.5, 24.0 and 24.0 m/s, respectively.

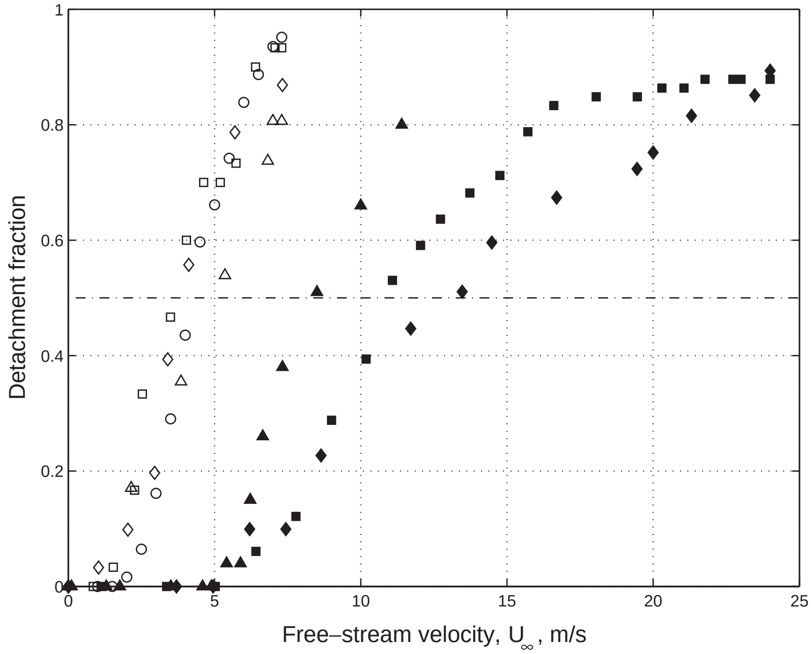

Fig. 2. Effects of the relative humidity: 18% (◇), 25% (□), 30% (○), 36% (△), 48% (▲), 61% (■) and 67% (◆). There was no residence time, the mean flow acceleration was 0.18 m/s^2, N_0 was about 0.5 particles/mm^2 and the flow was turbulent.

Ibrahim et al. (2003) estimated the free-stream velocities needed for detachment under lift-off, sliding, and pure rolling conditions. They considered the effects of surface roughness on adhesion and showed that the measured U_{th}'s correspond to incipient motion occurring as pure rolling. Consequently, their data suggest that detachment occurs when the moment of the aerodynamic drag force overcomes the moment of the rough pull-off force. The moments of the gravity and aerodynamic lift forces are negligible for the size range they considered. Accordingly, the pull-off force can be estimated from the measured U_{th}. Fig. 3 presents this estimation for two cases. The first case (solid symbols) corresponds to a drag force at the time of incipient motion calculated with a velocity more than the mean due to the existence of a burst-sweep event (for example, see Robinson, 1991). The second case (open symbols) considers only the drag force based on the mean flow velocity and ignores any possible causality between the particle detachment and the burst-sweep events. The estimated increase of the pull-off force with the relative humidity follows the same trend as in the published measurements in the literature. However, direct comparison is not feasible because many of the parameters of the pull-off force measurements, such as surface roughness and energy of adhesion, do not match those of the current experiments.

The bursts have been first observed by Kline, Reynolds, Schraub, and Runstadler (1967). The process begins with elongated counter-rotating stream-wise vortices that occur randomly in space and time. These subsequently cause near-wall fluid burst and sweep events (Corino & Brodkey, 1969).

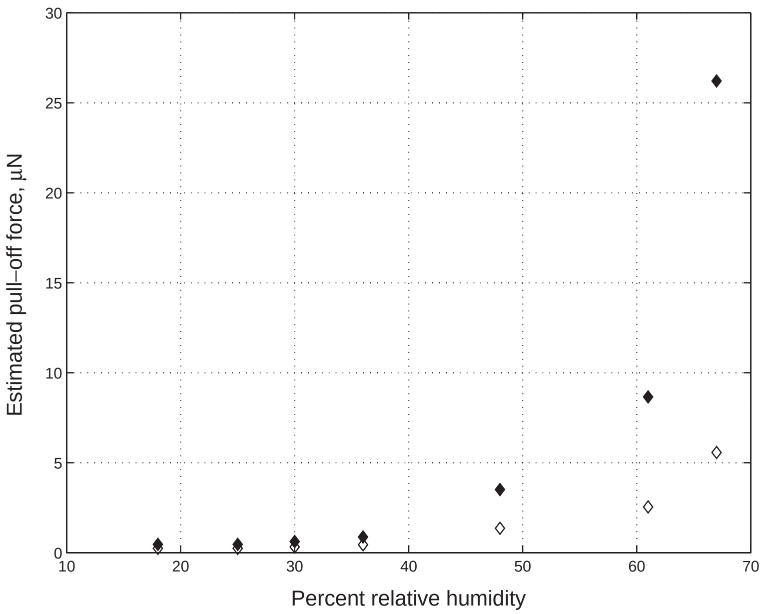

Fig. 3. Estimated pull-off forces at different relative humidities. Considering burst-sweep events (solid symbols) and without considering these events (open symbols).

In the ejection part, $\grave{u} < 0$, $\grave{w} > 0$ and in the sweep part $\grave{u} > 0$, $\grave{w} < 0$, where $\grave{u}$ and $\grave{w}$ are the stream-wise and normal velocity fluctuations, respectively.

As the relative humidity increases, the effective contact area increases resulting in a lower equivalent standard deviations of asperity heights and a higher ratio of rough-to-smooth pull-off forces. Using the estimated pull-off force and the results of Cheng et al. (2002), this trend is presented in Fig. 4.

3.2. Effects of residence time

The particle residence time on the surface has been found to affect the results, especially when the relative humidity is high. Fig. 5 shows measured behavior for different cases: in the first case, the deposition and the removal were made at a relative humidity of 30% and a residence time of about 24 h. The U_{th} is observed to increase from 4.2 m/s if there was no residence time to 5.5 m/s when the residence time was 24 h. In the second case, the deposition was made at a relative humidity of 61% and the removal was at a relative humidity of 30% with a residence time of 24 h. The U_{th} increased from 10.7 m/s if there was no residence time to more than 24 m/s when the residence time was 24 h. This observed increase in the U_{th} with the residence time when the relative humidity is high apparently is the result of the accumulation of water within the particle/surface interface and the corresponding increase in the true contact area.

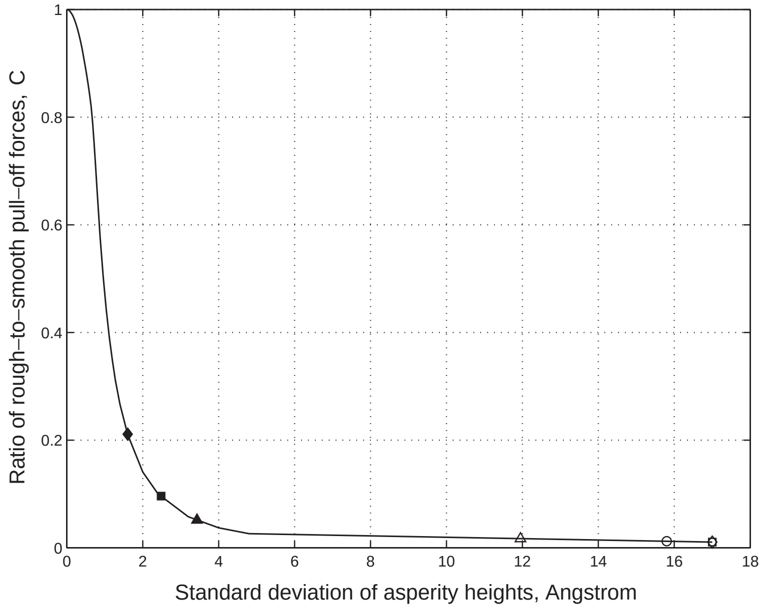

Fig. 4. Estimated decrease in the equivalent standard deviations of asperity heights (Å) versus the increase in rough pull-off force as the relative humidity increases. Solid curve: Theory of Cheng et al. (2002). Symbols: Estimations corresponding to the measurements shown in Fig. 2 for detachment with no burst-sweeps events.

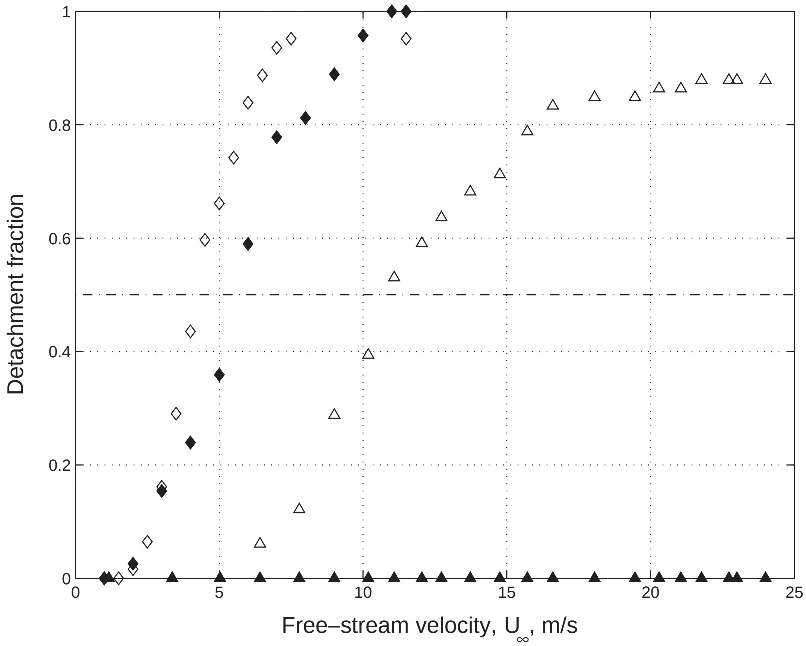

Fig. 5. Effects of residence time and relative humidity histories: Deposition and removal at 30% (◇), deposition and removal after 24 h at 30% (◆), deposition and removal at 61% (△), deposition at 61% and removal after 24 h at 30% (▲). The mean flow acceleration was 0.18 m/s^2, N_0 was about 0.5 particles/mm^2 and the flow was turbulent.

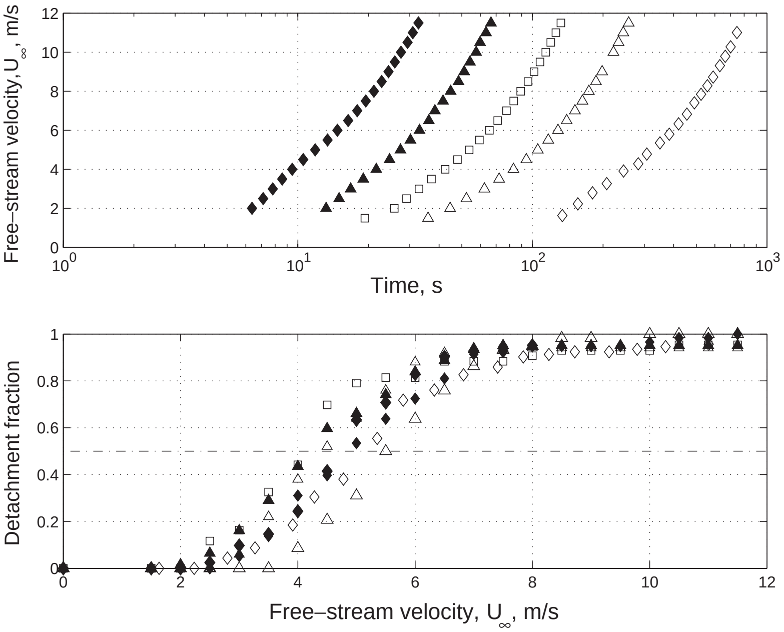

Fig. 6. Effects of the flow acceleration during the transient period, (m/s^2): 0.014 (◇), 0.045 (△, 2 experiments), 0.087 (□), 0.17 (▲), 0.34 (◆, 2 experiments). The relative humidity was 36%, no residence time, N_0 was about 0.5 particles/mm^2 and the flow was turbulent.

3.3. Effects of mean flow acceleration

Ibrahim et al. (2003) identified two distinct phases of detachment. The first was a short-term phase characterized by a high detachment rate and the second was a long-term phase characterized by a much lower detachment rate (about 500 times less). They related the transition between the two phases to the point at which the controlled free-stream velocity became constant. The present work investigates the effect of various mean flow accelerations on the detachment process during the short-term phase. Five values of mean flow acceleration were investigated, ranging from 0.014 to 0.34 m/s^2. To estimate the uncertainty, the experiments at 0.045 and 0.34 m/s^2 were repeated. Fig. 6 shows that the dependence of U_{th} on flow acceleration in the considered range is small and within the uncertainty of the measurements. The figure also reveals the progress of the transient free-stream velocity versus time. The data presented in Fig. 6 were made at a relative humidity of 36%. A similar result was obtained at higher free-stream velocities and a relative humidity of 61% and is given in Fig. 7.

3.4. Effects of deposition density and collisions

Depending on the relative magnitude of the aerodynamic drag, aerodynamic lift, pull-off, and gravity forces and moments, the particle may detach from the surface in direct lift-off, pure rolling, or sliding modes. If the particle moves along the surface after detachment, then particle–particle

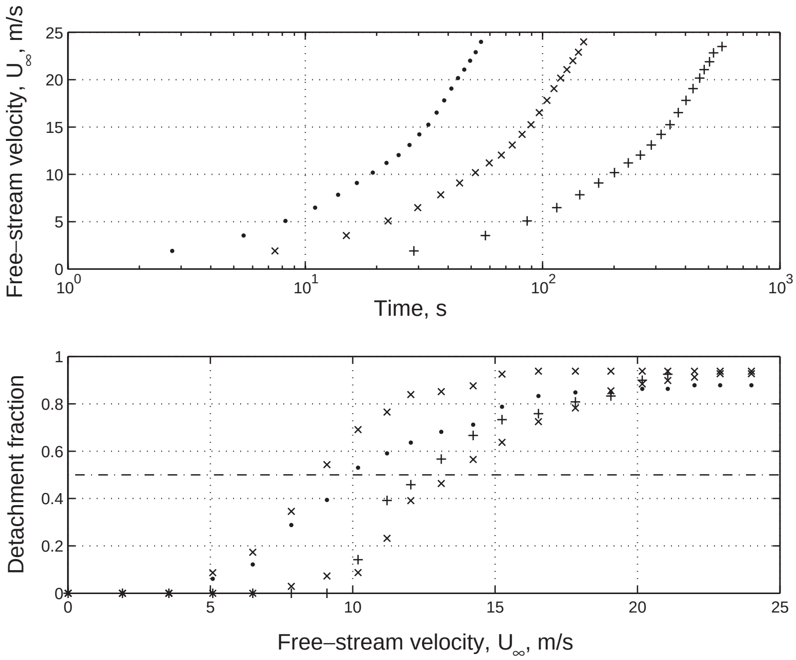

Fig. 7. Effects of the flow acceleration during the transient period, (m/s^2): 0.39 (●), 0.15 (X, 2 experiments), 0.042 (+). The relative humidity was 61%, no residence time, N_0 was about 0.5 particles/mm^2 and the flow was turbulent.

collisions can play a significant role in detaching other particles. The present experiments used relatively heavy particles (density of 8000 kg/m^3) and microvideographic observations showed that particles, within the filed of view, move *along* the surface after detachment and collide with other particles on the surface. Upon collision, the impacting particle supplies forces and moments to other particles that could overcome their adhesion. Eventually, they may detach and resuspend into the air flow. Many investigators studied the increase in resuspension due to non-central collisions by microparticles of different size. Fairchild and Tillery (1982) found that the resuspension rate for 7 μm count-median-diameter microspheres at a U_∞ of 10.5 m/s was increased by factors of 1.33 and 2.3 when 100 and 200 μm diameter spheres were injected upstream. They also found an increase in the maximum vertical flux of the 7 μm-diameter microspheres. The present work investigates the central impact process within the same diameter particles, which is due solely to the increased deposition density of the particles on the surface and subsequent collisions effects.

It is expected that the collisions mechanism will be more efficient than the fluid flow alone in detaching particles under some conditions. These conditions are that the density of the particles is much more than the air, that the particles detach at a velocity large enough such that the detaching moment supplied by the colliding particles is much more than that of a similar volume of air, and that there are enough particles to start many chains of collisions.

In the present work, two experiments were made corresponding to N_0 of approximately 0.5 and 3 particles/mm^2. The results of these cases are shown in Fig. 8. Particles removed by collisions were

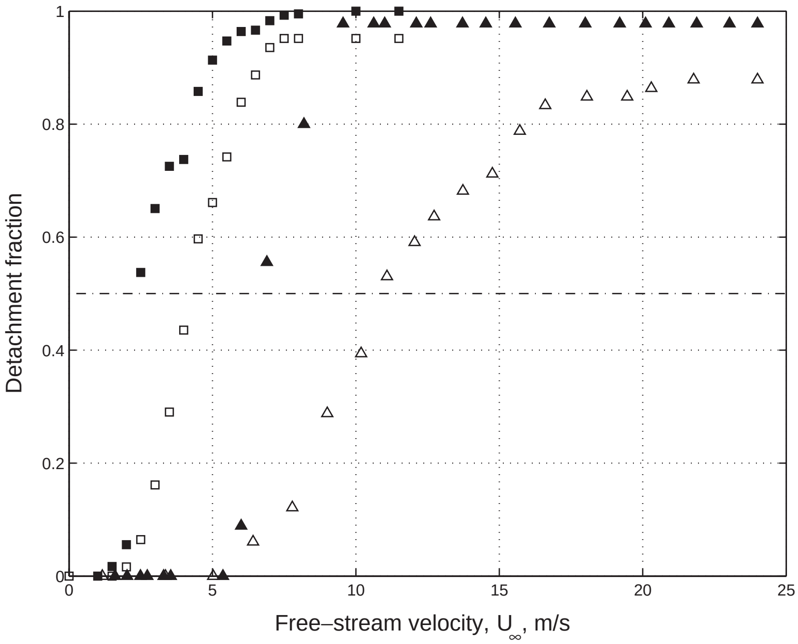

Fig. 8. Effects of the deposition density: At a relative humidity of 30% and a deposition density of about 0.5 particle/mm^2(□) and a deposition density of about 3 particle/mm^2(■); at a relative humidity of 61% and a deposition density of about 0.5 (△) and N_0 of about 3 (▲). The mean flow acceleration was 0.18 m/s^2 and the flow was turbulent.

included in the manual count. The U_{th} decreased from 4.2 to 2.5 m/s when the relative humidity was 30% and from 10.7 to 6.5 m/s when the relative humidity was 61%. This demonstrates that the collision mechanism can be very effective in detaching particles. At high deposition density, the U_{th} effectively decreases from the free-stream velocity needed for detaching 50% of the particles to the velocity needed to detach approximately 10% of them. This is due to the fact that once about 10% of the particles have detached, they trigger a large number of collisions that detach other particles.

The results for 70 μm diameter particles show that the collision mechanism amounts to removal of approximately 7% of the total detachment at N_0 of 0.5 micropartilce/mm^2 (where the particles projected area over the field's of view area is about 0.2%) and to approximately 90% of the total detachment when N_0 is about 3 particles/mm^2 (where the particles projected area over the field of view area is approximately 1.2%).

For particles of relatively high density such as stainless steel (8000 kg/m^3), almost every collision resulted in detachment as opposed to sticking. The exception was for a very small fraction of the particles that detach at a free-stream velocity less than about 1 m/s, which resulted in sticking rather than in detaching.

The question of how many particles should be considered to generate acceptable statistical accuracy was addressed. Fig. 9 shows the detachment fraction versus the free-stream velocity for two similar experiments at a U_∞ of 11.5 m/s, a relative humidity of 18%, and an initial number of particles of

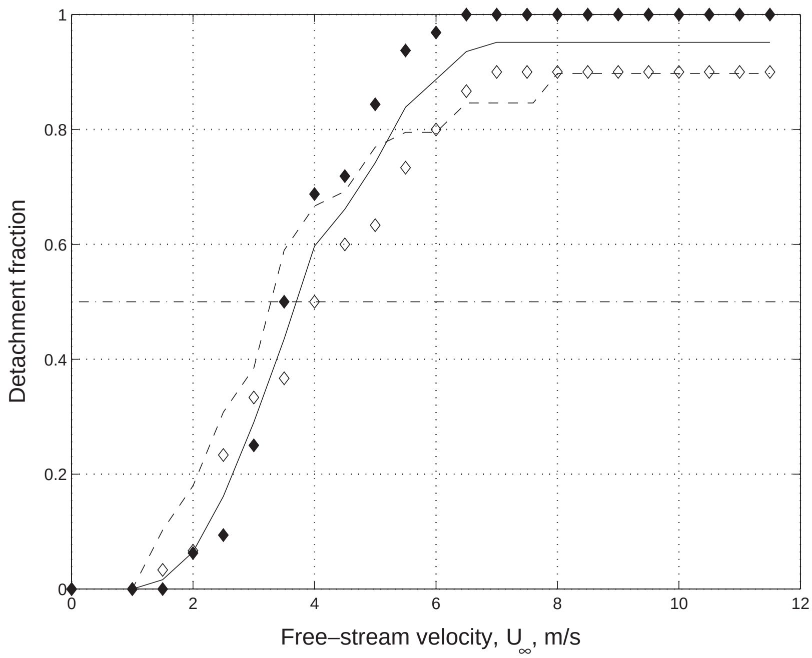

Fig. 9. Experimental determination of the number of particles needed to achieve a statistically accurate result: 39 particles (dotted curve), 62 particles (solid curve). The field of view of the 62 particles run is recounted: Left half only (◇), right half only (◆). The relative humidity was 18%, no residence time, the mean flow acceleration was 0.18 m/s^2 and the flow was turbulent.

39 particles for the first run (dotted curve) and 62 particles for the second (solid curve). During the analysis of the results of the second experiment, the field of view was divided into two parts of equal area. The division line was parallel to the flow direction. Then, the manual count of the particles in the second run was repeated. The open symbols show the results for the left half *only* (30 particles) and the solid symbols show the results for the right half *only* (32 particles). The figure reveals that the U_{th} for all three cases are within ±6% of the average, which is less than the overall uncertainty. This implies that approximately 30–40 particles are enough to yield a statistically accurate result for the case considered.

3.5. *Effects of final free-stream velocity*

Seven different final flow velocities were studied, ranging from 2.0 to 24 m/s at a relative humidity of 30%. The results are presented in Fig. 10. It is seen that the final free-stream velocity, U_∞, does not affect U_{th} to within the uncertainty of the measurements as long as the latter is smaller than the former. However, as the particles are subjected to smaller U_∞'s, the removal moments decrease, corresponding to a smaller final detachment fraction. For example, the final detachment fraction decreases from 0.94 at U_∞ of 7.5 m/s to 0.45 at U_∞ of 3.5 m/s.

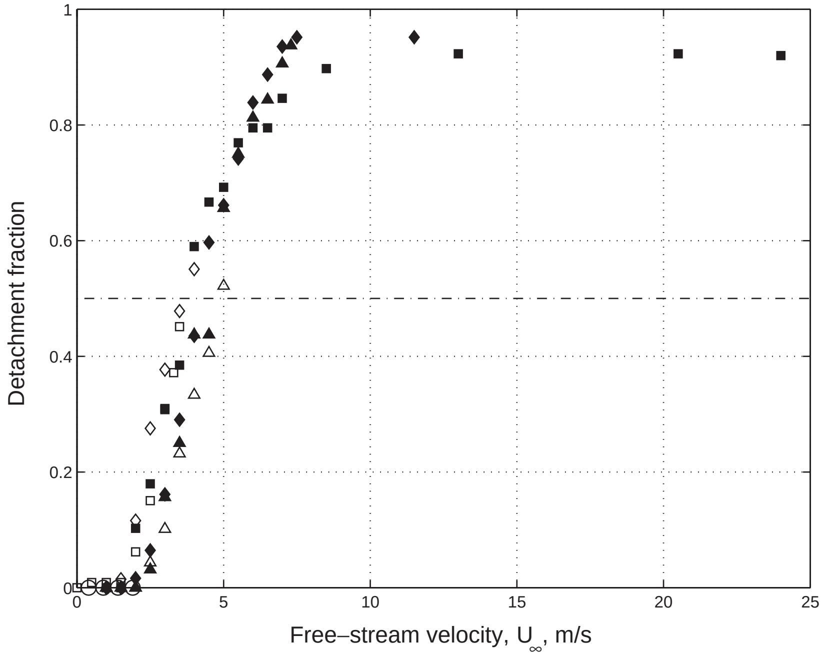

Fig. 10. Effects of the final free-stream velocity, U_∞, in m/s: 2.0 (◯), 3.5 (□), 4.2 (◇), 5.1 (△), 7.5 (▲), 12.5 (◆), and 24 (■). The relative humidity was 30%, no residence time, the mean flow acceleration was 0.18 m/s^2, N_0 was about 0.5 particles/mm^2 and the flow was turbulent.

3.6. Effects of final Reynolds number

The detachment process depends basically on the near-wall flow in the vicinity of the particles. Whether the flow is turbulent or laminar affects the wall shear stress and the flow structures near the wall and, consequently, detachment. All the aforementioned experiments were made under turbulent flow conditions, corresponding to a final Reynolds number of 1.05 E6. Another run was conducted in the same facility under laminar flow conditions, corresponding to a final Reynolds number of 1.05 E5, to investigate the effects of a different flow conditions on detachment.

The results of two cases, both at a relative humidity of 48% and a U_∞ of 24.0 m/s, are given in Fig. 11. The open symbols refer to the turbulent case and the solid symbols refer to the laminar case. It is observed that the U_{th} increases from 8.2 m/s (u^* of 0.37 m/s) in the turbulent case to 17.7 m/s (u^* of 0.51 m/s) in the laminar case.

This result was studied further using the model presented by Ibrahim et al. (2003). For the U_{th} measured under turbulent flow, the value of the parameter C can be estimated in order to match the measured U_{th} for the turbulent case. This value is 0.115 or 0.045, for detachment with and without burst-sweep events, respectively. Using these two values for C and estimating the drag force based on laminar flow, the estimated U_{th} for the laminar case are 15.6 and 10.3 m/s ($u^* = 0.46$ and 0.34 m/s), for detachment with and without burst-sweep events. The value of U_{th} of 15.6 m/s

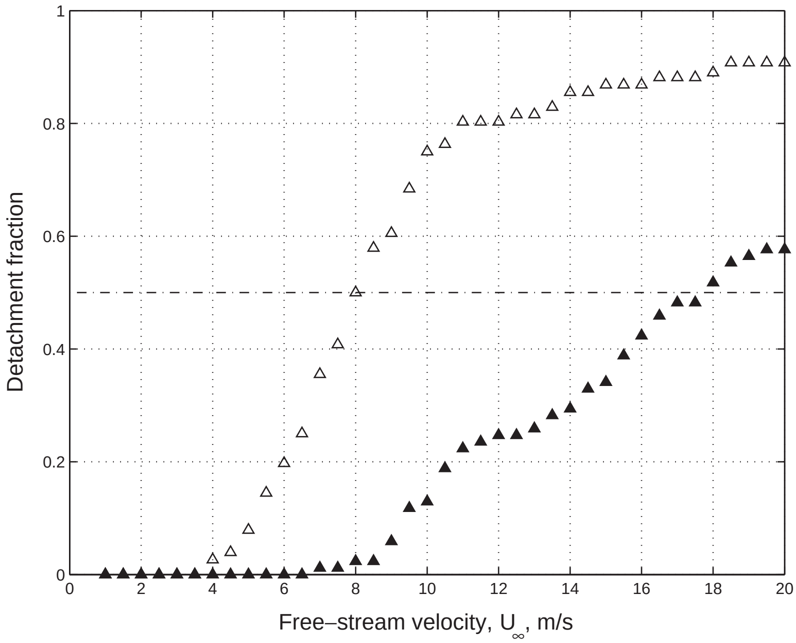

Fig. 11. Effects of the final Reynolds number: Turbulent flow (△, $Re = 1.05$ E6), Laminar flow (▲, $Re = 1.05$ E5). The relative humidity was 48%, no residence time, the mean flow acceleration was 0.18 m/s^2 and N_0 was about 0.5 particles/mm^2.

agrees to within uncertainty with the measured value of 17.7 m/s. This analysis supports the use of the model for laminar and humid cases. It further indicates that the increase in the U_{th} from the turbulent to the laminar case can be explained by the decreased wall shear stress at the wall in addition to the absence of burst-sweep events. This also suggests that a burst-sweep event was likely related to the detachment in the turbulent case.

3.7. Uncertainty in the U_{th}

The uncertainty in detachment experiments typically is large. This work presents a set of experimental data that lead to relatively small variability. Experimental variability was assessed by repeating the experiment under the same conditions. Fig. 12 shows the detachment fraction versus free-stream velocity for four experiments repeated under the same conditions. The uncertainty in the U_{th} typically is in the range from ±10% to 20%. This relatively low level of uncertainty was obtained by controlling the experimental conditions, which included the mean flow acceleration during the transient period, the relative humidity and the residence time, the deposition density, the final free-stream velocity and Reynolds number, the surface preparation technique and the particle counting technique. This variability results from the inherent scatter in particle/surface properties and the random nature of the turbulent flow.

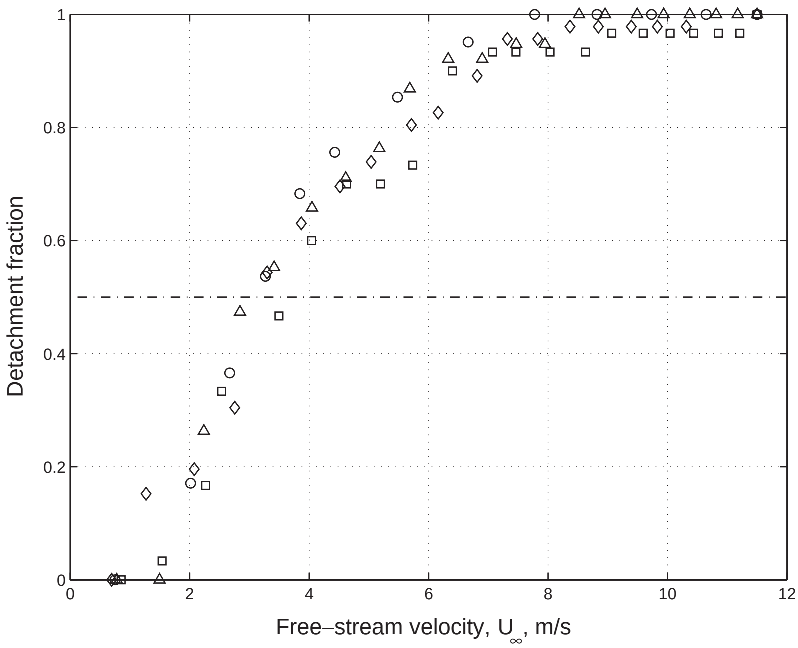

Fig. 12. Typical variability in the results under controlled experimental conditions. Different symbols refer to experiments repeated under the same conditions. The relative humidity was 25%, no residence time, the mean flow acceleration was 0.18 m/s^2, N_0 was about 0.5 particles/mm^2 and the final Reynolds number was 1.05 E6.

4. Summary and conclusions

Quantitative experimental results of the detachment of stainless-steel microspheres from glass substrates were presented. Surface-resident particles were exposed to an accelerating flow for a period of time, then to a constant velocity thereafter. Quantitative results about the dependence of U_{th} on relative humidity, residence time and different histories of relative humidity, flow acceleration in the transient period, deposition density of the particles on the surface and final free-stream velocity and Reynolds numbers were presented.

The increase in the U_{th} and the corresponding modelled increase in the pull-off force with relative humidity were presented. The increase in the U_{th} with residence time, especially at high relative humidity was highlighted. The role of the collision mechanism as a much more efficient detachment mechanism was indicated.

The deposition density factor was found to be the most effective factor that can enhance detachment at all relative humidities, and the residence time factor was found to be the most effective factor that can suppress detachment at high relative humidity. Within uncertainty limits, the mean flow acceleration in the transient period was found not to affect the U_{th} in the range from 0.014 to 0.34 m/s^2. The final free-stream velocity did not affect the U_{th} either, as long as it exceeded U_{th}. However, its effect on the final detachment fraction could not be ignored. An increase in the U_{th} was observed when the flow changed from turbulent to laminar. This change in the U_{th} can be explained by the decreased wall shear stress at the wall and the absence of the burst-sweep events.

Table 2
Summary of factor effects on U_{th}.

Factor	Factor change	U_{th} Change (m/s)	Factor held constants	Figure no.
Relative humidity RH (%)	18–67	3.6–13.4	$\tau_R \approx 0$ h, $\alpha = 0.18$ m/s^2 $N_0 \approx 0.5$ and turbulent flow	2
Residence time τ_R (h)	0–24	10.7 to > 24.0	61% RH, $\alpha = 0.18$ m/s^2 $N_0 \approx 0.5$ and turbulent flow	5
	0–24	4.2–5.5	30% RH, $\alpha = 0.18$ m/s^2 $N_0 \approx 0.5$ and turbulent flow	5
Acceleration α (m/s^2)	0.014–0.34	None	36% RH, $\tau_R = 0$ h, $N_0 \approx 0.5$ and turbulent flow	6
Initial number density N_0 (particles/mm^2)	≈ 0.5 to ≈ 3.0	10.7–6.5	61% RH, $\tau_R \approx 0$ h, $\alpha = 0.18$ m/s^2 and turbulent flow	8
Final free-stream Velocity, U_∞ (m/s)	2–24	None (as long as $U_\infty > U_{th}$)	30% RH, $\tau_R \approx 0$ h, $\alpha = 0.18$ m/s^2, $N_0 \approx 0.5$ and turbulent flow	10
Reynolds number Re	1.05 E5 to 1.05 E6	8.0–17.8	48% RH, $\tau_R \approx 0$ h, $\alpha = 0.18$ m/s^2 and $N_0 \approx 0.5$	11

Finally, the concept of detachment through a balance of drag and rough-surface pull-off forces was extended to explain the results obtained under humid and laminar conditions.

The effects of the key factors on U_{th} are summarized in Table 2.

Acknowledgements

Research described in this article was supported by Philip Morris, USA, Incorporated.

References

Ando, Y. (2000). The effect of relative humidity on friction and pull-off forces measured on submicron-size asperity arrays. *Wear*, *238*, 12–19.

Caylor, M. J. (1993). *The impact of electrically charged microspheres with planar surfaces under vacuum conditions*. Ph.D. Dissertation, University of Notre Dame.

Cheng, W., Brach, R. M., & Dunn, P. F. (2002). Surface roughness effects on microparticle adhesion. *Journal of Adhesion*, *78*, 929–965.

Corino, E. R., & Brodkey, R. S. (1969). Visual investigation of the wall region in turbulent flow. *Journal of Fluid Mechanics*, *37*, 1–30.

Corn, M. J. (1961). The adhesion of solid particles to solid surfaces II. *Journal of the Air Pollution Control Association*, *11*, 566–575.

Corn, M., & Stein, F. (1965). Re-entrainment of particles from a plane surface. *American Industrial Hygiene Association Journal*, *26*, 325–336.

Fairchild, C. I., & Tillery, M. I. (1982). Wind tunnel measurements of the resuspension of ideal particles. *Atmospheric Environment*, *16*, 229–238.

Ibrahim, A. H., Dunn, P. F., & Brach, R. M. (2003). Microparticle detachment from surfaces exposed to turbulent air flow: Controlled experiments and modeling. *Journal of Aerosol Science*, *34*, 765–782.

Klebanoff, P. S. (1954). Characteristics of turbulence in a boundary layer with zero pressure gradient. *NACA Technical Report 1247*.

Kline, S. J., Reynolds, W. C., Schraub, F. A., & Runstadler, P. W. (1967). The structure of turbulent boundary layers. *Journal of Fluid Mechanics*, *30*, 741–773.

Nicholson, K. W. (1988). A review of particle resuspension. *Atmospheric Environment*, *22*, 2639–2651.

Podczeck, F., Newton, J. M., & James, M. B. (1997). Variations in the adhesion force between a drug and carrier particles as a result of changes in the relative humidity of the air. *International Journal of Pharmaceutics*, *149*, 151–160.

Quon, R. A., Ulman, A., & Vanderlick, T. K. (2000). Impact of humidity on adhesion between rough surfaces. *Langmuir*, *16*, 8912–8916.

Reeks, M. W., Reed, J., & Hall, D. (1988). On the resuspension of small particles by a turbulent flow. *Journal of Physics. D: Applied Physics*, *21*, 574–589.

Robinson, S. K. (1991). Coherent motions in the turbulent boundary layer. *Annual Review of Fluid Mechanics*, *23*, 601–639.

Schlichting, H. (1979). *Boundary layer theory*. New York: McGraw-Hill.

Sehmel, G. A. (1980). Particle resuspension: A review. *Environment International*, *4*, 107–127.

Wang, H. C. (1991). Reducing uncertainties in particle adhesion and removal measurements. In: K. L. Mittal (Ed.), *Particles on surfaces 3*: *Detection*, *adhesion and removal* (pp. 193–202). New York: Plenum Press.

Wen, H. Y., Kasper, G., & Udischas, R. (1989). Short and long term particle release from surfaces under the influence of gas flow. *Journal of Aerosol Science*, *20*, 923–926.

Zimon, A. D. (1980). *Adhesion of dust and powders*. New York: Consultants Bureau.

Ziskind, G., Fichman, M., & Gutfinger, C. (1995). Resuspension of particulates from surfaces to turbulent flows: Review and analysis. *Journal of Aerosol Science*, *26*, 613–644.